The 3rd Joint International Conference on Multibody System Dynamics
The 7th Asian Conference on Multibody Dynamics
June 30-July 3, 2014, BEXCO, Busan, Korea

Study of High-Speed Train Dynamics under Degraded Adhesion Conditions: an Innovative HIL Architecture for Full-Scale Roller-Rigs

Benedetto Allotta*, Roberto Conti*, Enrico Meli*, Luca Pugi*, Alessandro Ridolfi*

* Department of Industrial Engineering
University of Florence
via di S. Marta 3, 50100, Italy
[benedetto.allotta, roberto.conti, enrico.meli, luca.pugi, alessandro.ridolfi]@unifi.it

ABSTRACT

In this paper, an innovative Hardware In the Loop (HIL) architecture is presented to test braking on board subsystems on full-scale roller-rigs. The new approach is based on an innovative control strategy to reproduce a generic wheel-rail adhesion pattern on the roller-rig and particularly suitable for degraded adhesion conditions. The presented strategy is also implemented by the full-scale roller-rig of the Railway Research and Approval Center (RRAC) of Firenze-Osmannoro (Italy). A complete model of the HIL system has been developed based on the real characteristics of the components to validate the proposed approach. Results obtained from the simulation model have been compared to the experimental data provided by Trenitalia and relative to on-track tests performed in Velim, Czech Republic, with a UIC-Z1 coach equipped with a fully-working WSP system. The preliminary validation performed with the HIL model highlights the good performances of the HIL strategy in reproducing the complex interaction between degraded adhesion conditions and railway vehicle dynamics during the braking manoeuvre on the roller-rig.

1 Introduction

In high speed trains, the control of the longitudinal train dynamics is strongly influenced by on board subsystems, such as Wheel Slide Protection (WSP) braking devices. Particularly, the analysis of these systems at high speeds and under degraded adhesion conditions, strongly modifies the vehicle safety and stability. On-track tests are currently quite expensive in terms of infrastructures and vehicle management; consequently, to reduce these costs, Hardware in the Loop (HIL) systems (such as full-scale roller-rigs) are usually employed to investigate the performances of braking subsystems [1][2][3][4][5]. Nevertheless, the use of roller-rigs for the degraded adhesion simulation is still limited to few applications (see for example full-scale roller-rigs for the study of the wear [6], HIL systems for WSP tests [7] and full-scale roller-rigs for locomotive tests [8]) due to the wear of the rolling surfaces, caused by the high slidings between rollers and wheelsets. The effects on the system stability are not acceptable because they can create unsafe situations: the flange wear can lead to the vehicle derailment while the tread wear can produce hunting instability of the vehicle. Furthermore the wheel flats may generate unsafe vibrations of the vehicle on the roller-rig. Finally the wear of the rolling surfaces deeply affects the maintenance costs: the rollers have to be frequently turned or substituted. In this work, the authors present an innovative Hardware In the Loop (HIL) architecture to test braking on board subsystems on full-scale roller-rigs. The new control strategy allows the reproduction on the roller-rig of a generic wheel-rail adhesion pattern under degraded adhesion conditions (characterized by adhesion coefficient values equal or less than 0.10), reducing the wear effects of the classical HIL systems [9] [10]. The new control architecture is based on an impedance control algorithm, in which the mechanical impedance simulation of the vehicle upon the rail is performed. In particular, the roller motors are controlled to recreate, on the wheelsets, the same angular velocities, applied torques and tangential efforts (exchanged between wheelsets and rails) calculated by a reference virtual railway vehicle model. Therefore, the main advantage is the high real adhesion coefficient between rollers and wheelsets that is far higher than the simulated one (negligible sliding occurs between them).

The presented strategy is also implemented by the innovative full-scale roller-rig of the Railway Research and Approval Center (RRAC) of Firenze-Osmannoro (Italy), recently built by Trenitalia and owned by SIMPRO. The University of Florence is currently involved into the pre-testing activities of the RRAC of

Firenze-Osmannoro, and the research activity is on-going. The described strategy has been completely simulated in the Matlab-Simulink environment [11] through an accurate model of the whole HIL architecture. Each model component is modelled according to the real characteristics provided by Trenitalia. The proposed approach has been preliminarily validated through a comparison with the experimental data provided by Trenitalia and relative to on-track tests performed on a straight railway track (in Velim, Czech Republic) with a UIC-Z1 coach equipped with a fully-working WSP system [12][13][14]. This initial validation carried out through the HIL model highlights the good performances of the HIL strategy in reproducing on the roller-rig the complex interaction between degraded adhesion conditions and railway vehicle dynamics during the braking manoeuvre.

2 Modelling of the Firenze-Osmannoro HIL system

In this section the models of the HIL system presented in the previous section (both hardware and software parts) and of all the components of the HIL architecture will be explained in detail. The main elements of the architecture are the test-rig model, the virtual railway vehicle model, the controllers and the estimators. In this case, the test-rig is completely simulated both for the UIC-Z1 railway vehicle (3D vehicle model and WSP model) and for the roller-rig (roller-rig 3D model). An innovative 3D contact model especially developed by the authors for this kind of application is used [19]. The mechanical and electrical characteristics of the vehicle [12][13] and of the roller-rig [15] are directly provided by Trenitalia and RFI. The flow of the data among the model parts is shown in Figure 1.

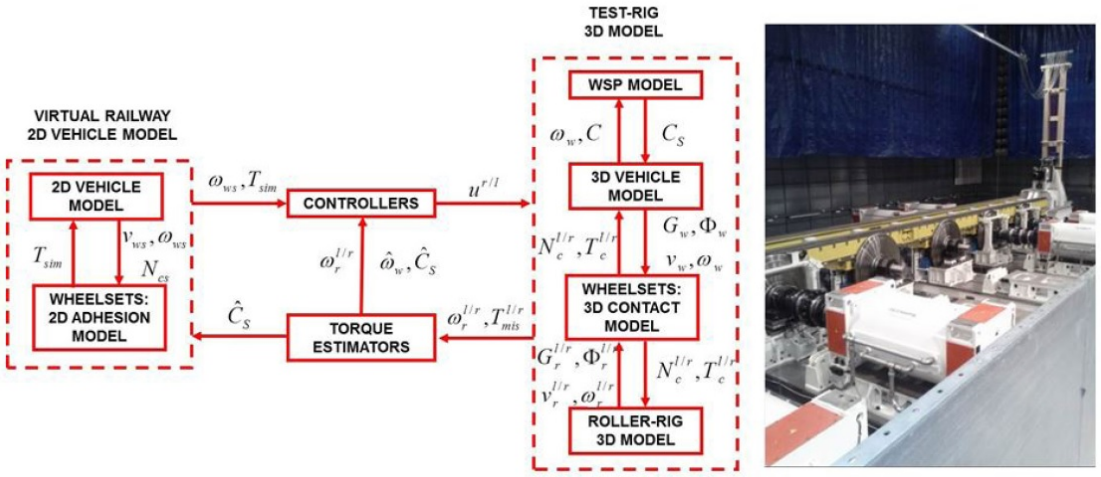

Figure 1. Interactions among the models of the various HIL architecture components

2.1 The test-rig model

The inputs of the whole test-rig model are the 8 roller control torques u^l, u^r (left and right) evaluated by the controllers to reproduce on the test-rig the same dynamical behaviour of the virtual railway model. The outputs are the 8 roller angular velocities ω_r^l, ω_r^r and the longitudinal reaction forces T_{mis}^l, T_{mis}^r measured on the roller supports. The test-rig model is composed of four parts (Figure 1). The considered railway vehicle is the UIC-Z1 wagon; its geometrical and physical characteristics are provided by Trenitalia S.p.A. [12]. The wagon is composed of one carbody, two bogie frames, eight axleboxes and four wheelsets. The primary suspension, including springs, dampers and axlebox bushings, connects the bogie frame to the four axleboxes while the secondary suspension, including springs, dampers, lateral bump-stops, anti-roll bar and traction rod, connects the carbody to the bogie frames. The multibody vehicle model takes into account all the degrees of freedom (DOFs) of the system bodies (one carbody, two bogie frames, eight axleboxes, and four wheelsets). Considering the kinematic constraints that link the axleboxes and the wheelsets (cylindrical

1DOF joints) and without including the wheel-rail contacts, the whole system has 50 DOFs. Both the primary suspension (springs, dampers and axlebox bushings) and the secondary suspension (springs, dampers, lateral bump-stops, anti-roll bar and traction rod) have been modelled through 3D visco-elastic force elements able to describe all the main non-linearities of the system. The non-linear elastic force elements have been modelled through non-linear functions that correlate the displacements and the relative velocities of the force elements connection points to the elastic and damping forces exchanged by the bodies. The inputs of the model are the 4 wheelset torques C_s modulated by the on board WSP and the contact forces calculated by the contact model, while the outputs are the kinematic wheelset variables transmitted to the contact model, the 4 original torques C (without the on board WSP modulation) and the 4 wheelset angular velocities ω_w. These last two outputs are not accessible by the HIL system. The WSP device installed on the UIC-Z1 coach [13][7] allows the control of the torques applied to the wheelsets, to prevent macro-sliding during the braking phase. The inputs are the braking torques C and the wheelset velocities ω_w, while the outputs are the modulated braking torques C_s. The WSP system working principle can be divided into three different tasks: the evaluation of the reference vehicle velocity V_{ref} and acceleration a_{ref} based on the wheelset angular velocities ω_w and accelerations $\dot{\omega}_w$; the computation of the logical sliding state $state_{WSP}$ (equal to 1 if sliding occurs and 0 otherwise)and the consequent torque modulation, through a speed and an accelerometric criterion and by means of a suitable logical table [7]; the periodic braking release to bring back the perceived adhesion coefficient to the original value (often used when degraded adhesion conditions are very persistent and the WSP logic tends to drift).

The 3D multibody model of the roller-rig [15] consists of 8 independent rollers with a particular roller profile able to exactly reproduce the UIC60 rail pattern with different laying angles α_p. The railway vehicle is axially constrained on the rollers using two axial links (front and rear) modelled by means of 3D force elements with linear stiffness and damping. The inputs of the test-rig model are the 8 torques u^l, u^r evaluated by the controllers and the contact forces calculated by the contact model; the outputs are the roller angular velocities ω_r^l, ω_r^r, the longitudinal reaction forces T_{mis}^l, T_{mis}^r measured on the roller supports and the kinematic wheelset variables transmitted to the contact model. The roller-rig actuation system consists of 8 synchronous motors, especially designed and developed in cooperation with SICME for this kind of application. The HIL architecture includes a direct-drive connection between the roller and the electrical machine. The synchronous motors have high efficiency associated with high torque density and flux weakening capability. Furthermore, to reach the dynamical and robustness performances required by the railway full-scale roller-rig, the motors are designed with a multilayer-rotor characterized by a high saliency ratio ξ and Interior Permanent Magnets (IPM). The IPM motors are controlled in real-time through vector control techniques; more particularly the vector control is a torque-controlled drive system in which the controller follows a desired torque. The main sensors installed on the roller-rig are the absolute encoders and the 3-axial load cells on the roller supports. These sensors are employed both in the torque estimators and in the controllers and measure, respectively, the roller angular velocities ω_r^l, ω_r^r and the longitudinal reaction forces T_{mis}^l, T_{mis}^r on the roller supports. The sensor characteristics are reported in [7]. The 3D contact model evaluates the contact forces $\mathbf{N_c^{l/r}}$, $\mathbf{T_c^{l/r}}$ for all the 8 wheel-roller pairs starting from the kinematic variables of the wheelsets and of the rollers: their positions $\mathbf{G_w}$, $\mathbf{G_r^{l/r}}$, orientations $\mathbf{\Phi_w}$, $\mathbf{\Phi_r^{l/r}}$, velocities $\mathbf{v_w}$, $\mathbf{v_r^{l/r}}$ and angular velocities $\omega_\mathbf{w}$, $\omega_\mathbf{r}^{\mathbf{l/r}}$. The contact model comprises three different steps. Firstly, all the contact points $\mathbf{P_c^{l/r}}$ of each wheel-roller pair are detected. Some innovative procedures have been recently developed by the authors [19]; the new algorithms are based on the reduction of the algebraic contact problem dimension through exact analytical techniques. Secondly, the normal contact problem is solved through the Hertz theory to evaluate the normal contact forces $\mathbf{N_c^{l/r}}$. Finally, the solution of the tangential contact problem is performed by means of the Kalker-Polach theory to compute the tangential contact forces $\mathbf{T_c^{l/r}}$. The contact model guarantees high accuracy and numerical efficiency; this way, the model can be implemented directly online inside the whole test-rig model. The main characteristics of the innovative procedure for the contact points detection can be summarized as follows:

1) it is a fully 3D algorithm that takes into account all the six relative DOFs between wheel and roller;

2) it is able to support generic wheel and roller profiles;

3) it assures a general and accurate treatment of the multiple contact without introducing simplifying assumptions on the problem geometry and kinematics and limits on the number of contact points detected;

4) it assures high numerical efficiency making possible the online implementation within the commercial multibody software without discrete Look-up Tables. [11]

2.2 The virtual railway vehicle model

The virtual railway vehicle model simulates the dynamical behaviour of the railway vehicle during a braking phase under degraded adhesion conditions. The model, designed for a real-time implementation, is composed of two parts: the 2D vehicle model and the 2D adhesion model. The inputs are the 4 estimated torques $\widehat{C}_s$ to be applied to the wheelsets while the outputs are the 4 simulated tangential contact forces T_{sim} and the 4 simulated wheel angular velocities ω_{ws}. The 2D vehicle model of the considered railway vehicle (UIC-Z1 coach) is a simplified 2D multibody model of the longitudinal train dynamics (only 3 DOFs for each body are taken into account) [12]. The model consists of a carbody, two bogies and four wheelsets, held by the primary and secondary suspensions. Starting from the estimated torques $\widehat{C}_s$, the model evaluates the kinematic variables of the 4 wheelsets v_{ws}, ω_{ws} and the 4 normal contact forces N_{cs} to be passed to the adhesion model and receives the 4 tangential contact forces T_{sim}. The adhesion model has been especially developed to describe degraded adhesion conditions [16][17] and calculates, for all the 4 wheelset-rail pair, the tangential contact forces T_{sim} starting from the wheelset kinematic variables v_{ws}, ω_{ws} and the normal contact forces N_{cs} (see Figure 2). The main phenomena characterising the degraded adhesion are the large

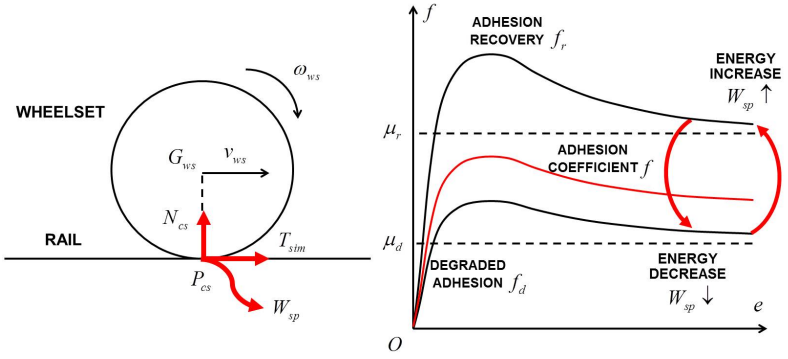

Figure 2. The adhesion model

sliding occurring at the contact interface and, consequently, the high energy dissipation. Such a dissipation causes a cleaning effect on the contact surfaces and finally an adhesion recovery due to the removal of the external contaminants. When the specific dissipated energy W_{sp} is low the cleaning effect is almost absent, the contaminant level h does not change and the adhesion coefficient f is equal to its original value f_d in degraded adhesion conditions f_d. As the energy W_{sp} increases, the cleaning effect increases too, the contaminant level h becomes thinner and the adhesion coefficient f raises. In the end, for large values of W_{sp}, all the contaminant is removed (h is null) and the adhesion coefficient f reaches its maximum value f_r; the adhesion recovery due to the removal of external contaminants is now completed. At the same time if the energy dissipation begins to decrease, due for example to a lower sliding, the reverse process occurs (see Figure 2). Since the contaminant level h and its characteristics are usually totally unknown, it is usefull trying to experimentally correlate the adhesion coefficient f directly with the specific dissipated energy W_{sp}:

$$W_{sp} = T_{sim}e = fN_{cs}e \quad f = \frac{T_{sim}}{N_{cs}} \tag{1}$$

To reproduce the qualitative trend previously described and to allow the adhesion coefficient to vary between the extreme values f_d and f_r, the following expression for f is proposed:

$$f = [1 - \lambda(W_{sp})]f_d + \lambda(W_{sp})f_r \tag{2}$$

where $\lambda(W_{sp})$ is an unknown transition function between degraded adhesion and adhesion recovery while the adhesion levels f_d, f_r can be evaluated according to [16][17] as a function of e, N_{cs} and the track friction coefficients μ_d, μ_r (corresponding to degraded adhesion and full adhesion recovery, respectively). The function $\lambda(W_{sp})$ has to be positive and monotonous increasing; moreover the following boundary conditions are supposed to be verified: $\lambda(0) = 0$ and $\lambda(+\infty) = 1$.

In the end, the desired values of the adhesion coefficient f and of the tangential contact force $T_{sim} = fN_{cs}$ can be evaluated by solving the non-linear algebraic Eq. (2) in which the explicit expression of W_{sp} has

been inserted (see Eq. (1)):

$$f = \Im(f, t) \tag{3}$$

where $\Im$ indicates the generic functional dependence. Due to the simplicity of the transition function $\lambda(W_{sp})$, the solution can be easily obtained through standard non-linear solvers.

2.3 The controllers

The controllers have to reproduce on the roller-rig the dynamical behaviour of the virtual railway vehicle under degraded adhesion conditions in terms of angular velocities ω_w, applied torques C_s and, consequently, tangential contact forces $T_c^{l/r}$. The inputs of the controller are the simulated tangential forces T_{sim}, the simulated wheelset angular velocities ω_{ws}, the estimated wheel angular velocities $\widehat{\omega}_w$, the estimated motor torques $\hat{C}_S$ and the roller angular velocities $\omega_r^{l/r}$. The outputs are the 8 roller control torques $u^{l/r}$.

The controller layout consists of 8 independent controllers (one for each roller) and makes use of a sliding mode strategy based on the dynamical equations of the roller rig; this way, it is possible to reduce the disturbance effects due to the system non-linearities and the parameter uncertainties [18]. The total control torques $u^{l/r}$ are defined as:

$$u^{l/r} = u_{cont}^{l/r} + u_{disc}^{l/r} + u_{diff}^{l/r} \tag{4}$$

where the continuous control part $u_{cont}^{l/r}$ is built starting from the approximated 1D models of wheelset and rollers and by supposing the slidings between the contact surfaces negligible (on the roller-rig the adhesion conditions are good, with a friction coefficient μ_{roll} equal to 0.3), $u_{disc}^{l/r}$ is the discontinuous control part related to the rejection of the disturbancies and $u_{diff}^{l/r}$ is an auxiliary control part aimed at synchronizing the roller angular velocities ω_r^l, ω_r^r.

2.4 The torque estimators

The estimators aim at evaluating the wheelset angular velocities $\widehat{\omega}_w$ and the torques applied to the wheelset $\widehat{C}_s$ starting from the roller angular velocities $\omega_r^{l/r}$ and the longitudinal reaction forces $T_{mis}^{l/r}$ on the roller supports. At this point, to estimate the motor torque applied to the wheelset, the estimator employes the simplified dynamical model of the wheelset:

$$\hat{C}_s = J_w \hat{\dot{\omega}}_w - \hat{T}_c^l r_w - \hat{T}_c^r r_w. \tag{5}$$

It is worth noting that, in this kind of applications, the estimators have to be necessarily simple because they are thought for a real-time implementation and, at the same time, the physical characteristics of the railway vehicle on the roller-rig are generally unknown.

3 Experimental data

The HIL model performance have been validated by means of the comparison with the experimental data, provided by Trenitalia S. p. A. [14] and coming from on-track braking tests carried out in Velim (Czech Republic) with the coach UIC-Z1 [12]. The considered vehicle is equipped with a fully-working WSP system [13]. These experimental tests have been carried out on a straight railway track. The wheel profile is the ORE S1002 (with a wheelset width d_w equal to $1.5\mathrm{m}$) while the rail profile is the UIC60 (with a gauge d_r equal to $1.435\mathrm{m}$ and a laying angle α_p equal to $1/20\mathrm{rad}$). The main characteristics of the braking test, considered as benchmark in this paper, are summarized in [7],[16]. The value of the kinetic friction coefficient under degraded adhesion conditions μ_{cd} depends on the test performed on the track; the degraded adhesion conditions are usually reproduced using a watery solution containing surface-active agents, e.g. a solution sprinkled by a specially provided nozzle directly on the wheel-rail interface on the first wheelset in the running direction. The surface-active agent concentration in the solution varies according to the type of test and the desired friction level. The value of the kinetic friction coefficient under full adhesion recovery μ_{cr} corresponds to the classical kinetic friction coefficient under dry conditions. Firstly the vehicle and wheelset velocities v^{sp}, $v_{wi}^{sp} = r_w \omega_{wi}^{sp}$ $(i = 1, ..., 4)$ are taken into account (see

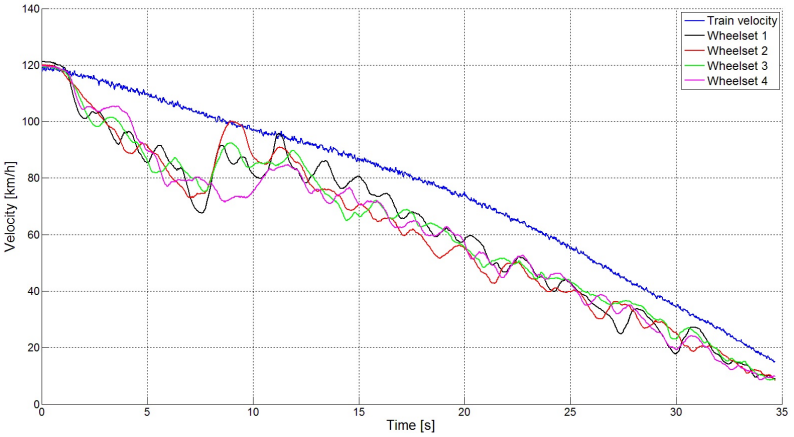

Figure 3. Experimental vehicle and wheelset velocities v^{sp}, $v_{wi}^{sp} = r_w \omega_{wi}^{sp}$

Figure 3). Both the WSP intervention and the adhesion recovery in the second part of the braking maneuver are clearly visible. Secondly the slidings among the wheelsets and the rails have been considered: $s_i^{sp} = v^{sp} - r_w \omega_{wi}^{sp} = v^{sp} - v_{wi}^{sp}$. However these physical quantities cannot be locally compared to each other because of the complexity and the chaoticity of the system due, for instance, to the presence of discontinuous and threshold elements like the WSP. To better evaluate the behaviour of s_i^{sp} from a global point of view, it is usefull to introduce the statistical means $\bar{s}_i^{sp}$ and the standard deviations Δ_i^{sp} of the considered variables $\bar{s}_i^{sp} = \frac{1}{T_F - T_I} \int_{T_I}^{T_F} s_i^{sp} dt$ and $\Delta_i^{sp} = \sqrt{\frac{1}{T_F - T_I} \int_{T_I}^{T_F} (s_i^{sp} - \bar{s}_i^{sp})^2 dt}$ where T_I and T_F are respectively the initial and final times of the simulation.

4 The model validation

In this chapter the whole HIL architecture model is simulated and validated. More in detail, both the dynamical and the control performances of the system will be analyzed. The main control and integration parameters are summarized in [19]. The simulated vehicle and wheelset velocities v_s, $v_{wsi} = r_w \omega_{wsi}$ are reported in Figure 4-(a). Figures 3 and 4-(a) highlight a good qualitative matching between experimental and simulated data, both concerning the WSP intervention and the adhesion recovery in the second part of the braking maneuver. The direct comparison between the experimental and simulated train velocities v^{sp}, v_s is illustrated in Figure 4-(b) and shows also a good quantitative agreement between the considered quantities. Subsequently, according to chapter 3, the simulated slidings among wheelsets and rails $s_{si} =$

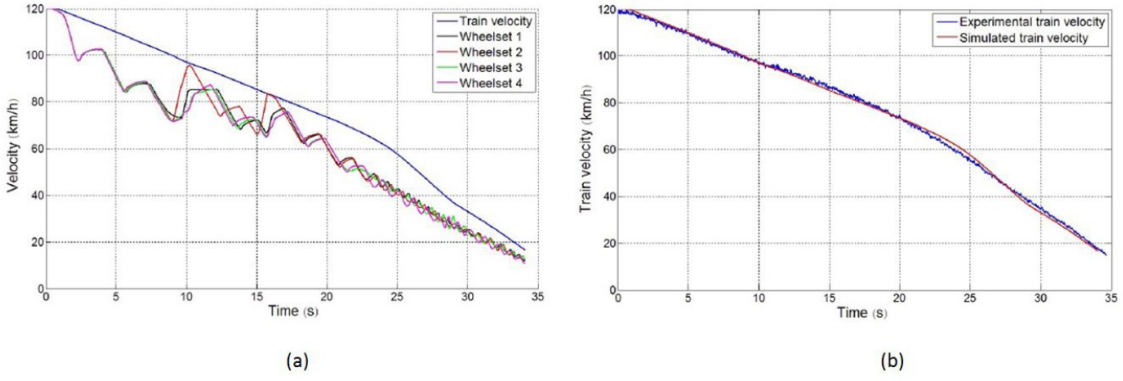

Figure 4. (a) Simulated vehicle and wheelset velocities v_s,$v_{wsi} = r_w \omega_{wsi}$ - (b) Experimental and simulated train velocities v^{sp}, v_s

$v_s - r_w \omega_{wsi} = v_s - v_{wsi}$ are taken into account and compared to the experimental ones s_i^{sp}. The matching

between experimental and simulated slidings is qualitatively good. However, since these physical quantities cannot be locally compared to each other because of the complexity and the chaoticity of the system, the statistical means $\bar{s}_{si}$ and the standard deviations Δ_{si} of the simulated slidings s_{si} are introduced to better evaluate the global behaviour of analyzed variables. The comparison between experimental $\bar{s}_i^{sp}$, Δ_i^{sp} and simulated $\bar{s}_{si}$, Δ_{si} statistical indices is reported in Table 1 and highlights also a good quantitative match between the studied quantities.

Table 1. Experimental $\bar{s}_i^{sp}$, Δ_i^{sp} and simulated $\bar{s}_{si}$, Δ_{si} statistical indices

Wheelset	$\bar{s}_i^{sp}$ (km/h)	$\bar{s}_{si}$ (km/h)	Δ_i^{sp} (km/h)	Δ_{si} (km/h)
Wheelset 1	13.08	12.82	6.45	6.56
Wheelset 2	13.36	12.88	7.25	6.95
Wheelset 3	13.09	13.32	5.92	5.70
Wheelset 4	13.52	13.59	6.22	5.82

The controller performances are evaluated in terms of angular velocity error $e_\omega = \omega_{ws} - \omega_w$ and the torque estimation error $e_c = \hat{C}_s - C_s$. Small values of the errors e_ω, e_c assure a good estimation of the tangential contact forces $T_c^{l/r}$. The time history of the angular velocity error e_ω is plotted in Figure 5-(a) and shows the control capabilty of stabilising the sistem and rejecting the disturbancies produced by the initial transient and the adhesion recovery in the second phase of the braking maneuvre.

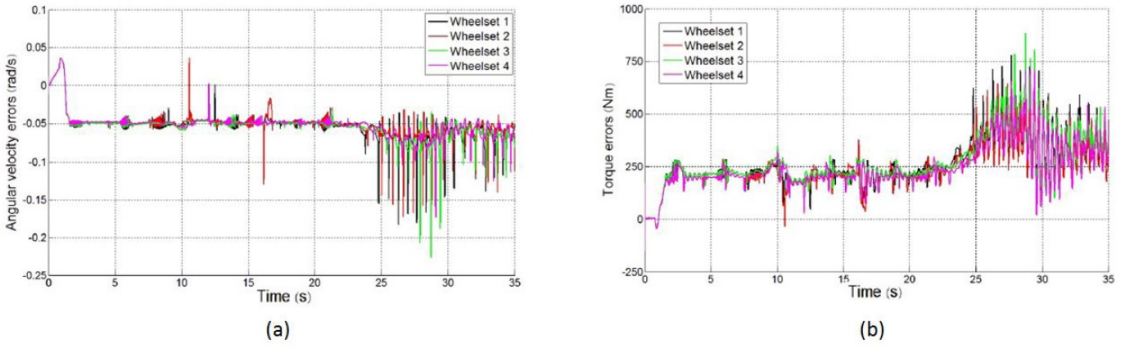

Figure 5. (a) Angular velocity error e_ω - (b) Torque estimation error e_c

The torque estimation error $e_c = \hat{C}_s - C_s$ is reported in Figure 5-(b). Also in this case the controlllers turn out to be effective in reproducing the real torques applied to the wheelsets of the vehicle.
Finally, the result analysis highlights the control capability of reproducing on the roller-rig a generic wheel-rail degraded adhesion pattern calculated by the reference virtual railway vehicle model (in terms of angular velocities ω_w, applied torques on the wheelsets C_s and, consequently, in terms of tangential efforts $T_c^{l/r}$ exchanged between the wheelsets and the rails).

5 Conclusions and further developments

In this paper, an innovative Hardware In the Loop (HIL) architecture to test braking on board subsystems has been described. The new control strategy is implemented for a full-scale roller-rig, permitting to simulate different wheel-rail adhesion patterns (particularly degraded adhesion conditions). The results obtained during this preliminary research activity have highlighted good performances in reproducing on the roller-rig the complex interaction between degraded adhesion conditions and railway vehicle dynamics, especially during braking manoeuvres. The innovative approach has been preliminarily validated through experimental data provided by Trenitalia.

The results from the simulation model have been compared to the experimental data provided by Trenitalia and relative to on-track tests performed in Velim, Czech Republic, with a UIC-Z1 coach equipped with a fully-working WSP system. The main industrial results concerning the new architecture are the reduction of the expensive on-track tests and the possibility to test several on board subsystems on a roller-rig both with a well specified adhesion conditions.

The future developments of this research activity are scheduled and will regard the implementation both of the control strategy and of the virtual vehicle model on the full-scale roller-rig recently built in the Railway Research and Approval Center (RRAC) of Firenze-Osmannoro (Italy). Finally, a further validation of the proposed HIL approach will be possible through experimental tests directly performed on the roller-rig.

REFERENCES

[1] Jaschinki, A.; Chollet, H.; Iwnicki, S.: The application of the roller rigs to railway vehicle dynamics. Vehicle System Dynamics. 1999;31:325-344.

[2] Dukkipati, R.: A parametric study of the lateral stability of a railway bogie on a roller rig. Proceedings of the Institution of Mechanical Engineering Part F. 1999;213:39-47.

[3] Ahn, K.; Park, J.; Ryew, S.: The construction of a full-scale wheel/rail roller rig in Korea. Proceedings of the IEEE International Conference on Automation Science and Engineering (CASE); 2012.

[4] Lee, N.; Kang, C.; Lee, W.; Dongen, T.: Roller rig tests of a semi-active suspension system for a railway vehicle. Proceedings of the IEEE International Conference on Control, Automation and Systems (ICCAS); 2012.

[5] Dukkipati, R.: Lateral stability analysis of a railway truck on roller rig. Mechanism and Machine Theory. 2001;36:189-204.

[6] Zhang, W.; Chen, J.; Wu, X.; Jin, X.: Wheel/rail adhesion and analysis by using full scale roller rig. Wear. 2002;253:82-88.

[7] Allotta, B.; Conti, R.; Malvezzi, M.; Meli, E.; Pugi, L.; Ridolfi, A.: Numerical simulation of a HIL full scale roller-rig model to reproduce degraded adhesion conditions in railway applications. Proceedings of the ECCOMAS 2012 Congress; 2012.

[8] Malvezzi, M.; Allotta, B.; Pugi, L.: Feasibility of degraded adhesion tests in a locomotive roller rig. Proceedings of the Institution of Mechanical Engineering Part F. 2008;222:27-43.

[9] Auciello; J.; Ignesti, M.; Malvezzi, M.; Meli, E.; Rindi, A.: Development and validation of a wear model for the analysis of the wheel profile evolution in railway vehicles. Vehicle System dynamics. 2012;50:1707-1734.

[10] Ignesti, M.; Innocenti, A.; Marini, L.; Meli, E.; Rindi, A.: Development of a wear model for the wheel profile optimisation on railway vehicles. Vehicle System dynamics. 2013;51:1363-1402.

[11] Official Site of Mathworks. www.mathworks.com. Natick, MA: 2013.

[12] Trenitalia SpA. UIC-Z1 coach. Internal Report of Trenitalia; 2000.

[13] Trenitalia SpA. WSP system. Internal Report of Trenitalia; 2005.

[14] Trenitalia SpA. On-track braking tests. Internal Report of Trenitalia; 2006.

[15] Trenitalia SpA. Full-scale roller-rig: technical documentation. Internal Report of Trenitalia; 2011.

[16] Allotta, B.; Meli, E.; Ridolfi, A.; Rindi, A.: Development of an innovative wheel–rail contact model for the analysis of degraded adhesion in railway systems. Tribology International. 2013;69:128-140.

[17] Meli, E.; Ridolfi, A.: An innovative wheel–rail contact model for railway vehicles under degraded adhesion conditions. Multibody System Dynamics. 2013; doi:10.1007/s11044-013-9400-9.

[18] Khalil, H.K.: Nonlinear Systems. United States: Prentice Hall; 2002.

[19] Conti, R.; Meli, E.; Pugi, L.; Malvezzi, M.; Bartolini, F.; Allotta, B.; Rindi, A.; Toni, P.: A numerical model of a HIL scaled roller rig for simulation of wheel-rail degraded adhesion condition. Vehicle System Dynamics. 2012;50: 775-804.